Vol 16 No 9, September 2007
1009-1963/2007/16(09)/2791-07

Chinese Physics

© 2007 Chin. Phys. Soc.
and IOP Publishing Ltd

Electronic structure and optical properties of In-doped $SrTiO_3$ by density function theory*

Zhang Zhi-Yong(张志勇)[a)†], Yun Jiang-Ni(贠江妮)[a)], and Zhang Fu-Chun(张富春)[a)b)]

[a)] *Information Science and Technology Institution, Northwest University, Xi'an* 710069, *China*
[b)] *College of Physics & Electronic Information, Yan'an University, Yan'an* 716000, *China*

(Received 19 December 2006; revised manuscript received 28 February 2007)

The effect of In doping on the electronic structure and optical properties of $SrTiO_3$ is investigated by the first-principles calculation of plane wave ultra-soft pseudo-potential based on the density function theory (DFT). The calculated results reveal that due to the hole doping, the Fermi level shifts into valence bands (VBs) for $SrTi_{1-x}In_xO_3$ with $x = 0.125$ and the system exhibits p-type degenerate semiconductor features. It is suggested according to the density of states (DOS) of $SrTi_{0.875}In_{0.125}O_3$ that the band structure of p-type $SrTiO_3$ can be described by a rigid band model. At the same time, the DOS shifts towards high energies and the optical band gap is broadened. The wide band gap, small transition probability and weak absorption due to the low partial density of states (PDOS) of impurity in the Fermi level result in the optical transparency of the film. The optical transmittance of In doped $SrTiO_3$ is higher than 85% in a visible region, and the transmittance improves greatly. And the cut-off wavelength shifts into a blue-light region with the increase of In doping concentration.

Keywords: the density function theory, $SrTiO_3$, In-doping, electronic structure, optical transmittance

PACC: 7115M, 7125, 7155, 7850

1. Introduction

Strontium titanate ($SrTiO_3$), a typical perovskite material, has attracted much attention due to the interest in fundamental research and its potential applications in fields of ferroelectricity, grain-boundary barrier layer capacitors, oxygen-gas sensors, epitaxial growth substrates for high temperature superconductor thin films, optical switches and so on.[1−4] It is well known that stoichiometric $SrTiO_3$ is a good insulator with a band gap of about 3.2 eV at room temperature. But its conductivity can be induced either through the reduction of oxygen ($SrTiO_{3-x}$) or through impurity doping, which has important applications in oxide devices[5] as well as in the theoretical and experimental investigations of $SrTiO_3$.[6−10]

The behaviour of doped $SrTiO_3$ has been widely studied in an attempt to understand the rich variations in physical properties arising from carrier doping.[8−13] It has been found that $SrTiO_3$ exhibits n-type conductivity on substituting Nb^{5+} (or La^{3+}) for Ti^{4+} (or Sr^{2+}) and it becomes a superconductor at $T_c = 0.3$ K. Also the n-type doped system has been used in practical applications such as electrodes and gas sensors. The p-type $SrTiO_3$ will be a very promising material. First, it can be used as wide-gap semiconductor diodes in a blue-light region, so it is highly valued in semiconductor industries. Second, it is well known that p-type doping in perovskite structure can accommodate the protonic conductivity.[14,15] And the protonic conductors are important materials for a wide range of electrochemical applications such as fuel cells and hydrogen sensors in the renewable energy source industries. To our knowledge, however, the investigation on p-type doped $SrTiO_3$ is little made both experimentally and theoretically. Higuchi *et al*[14] experimentally have reported the electronic structure of a p-type $SrTiO_3$ single crystal in which the acceptor ion Sc^{3+} is introduced into the Ti^{4+} site. And the effect of Sc^{3+} on the electronic properties has been studied by Weidong Luo *et al*[11] using *ab initio* pseudo-potential density function theory. Moreover, Shouyu Dai *et al*[13] have found that $SrTiO_3$ exhibits p-type conductivity when doped by the substitution of In for Ti in experiment. There has been no theoretical investigation on In doped $SrTiO_3$ so far. So it is necessary to use the first principles method to explore the effect of p-type doping In on the electronic

*Project supported by the Natural Science Foundation of Shaanxi Province, China (Grant No 2005F06).
†Corresponding author. E-mail: zhangzy@nwu.edu.cn

structure of $SrTiO_3$.

In this paper, we perform the first principles calculation of the electronic structure of $SrTi_{1-x}In_xO_3$ for the cases of $x = 0.0$, 0.125 and 0.25 by the CASTEP software package[16] based on density function theory (DFT) in a supercell approach. Since the supercell approach is time-consuming, we have to construct a supercell of eight unit cells comprising at most 40 atoms.

2. Computational details

$SrTiO_3$ has an ideal cubic perovskite–type structure at room temperature. It belongs to the space group $Pm3m(O_{h1})$, with the Sr atom sitting at the origin point, Ti at the body centre and three oxygen atoms at the three face centres, and its lattice constant is $a = b = c = 0.3905$ nm. The unit cell contains one formula unit of $SrTiO_3$. In order to study fractional In substitution, it is necessary to consider a larger cell than the basic unit. In our computation, we take three In concentrations: $SrTiO_3$, $SrTi_{0.875}In_{0.125}O_3$ and $SrTi_{0.75}In_{0.25}O_3$, and all calculations are performed by using a $2 \times 2 \times 2$ supercell.

In the case of the substitution of a single In atom for Ti atoms ($SrTi_{0.875}In_{0.125}O_3$), there is no difference between configurations with the In atom at different Ti sites in the supercell. However, the situation becomes complicated with two In atoms in the supercell. There are three different ways of distributing the two In atoms in the supercell, distinguished between each other by the relative positions of the two In atoms. The three distinct configurations (A–C) are shown in Fig.1 where the In–In separation is descending, and the distance between the two In atoms corresponding to each configuration is listed in Table 1. Because the distance between the two In atoms in configuration A is the largest, we only study this configuration to ensure that there is a weak interaction between the In impurity atoms.

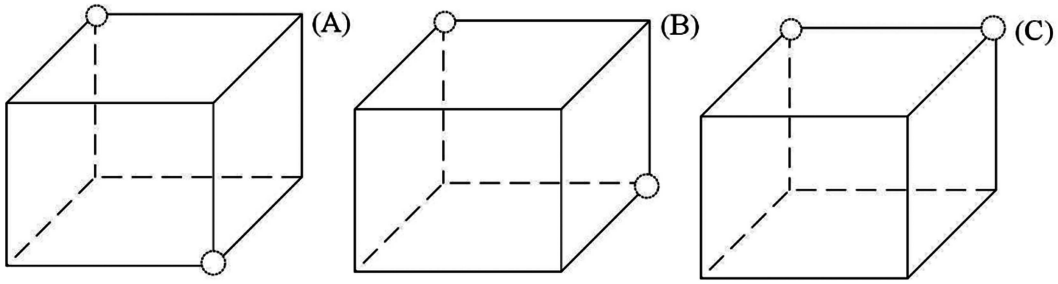


Fig.1. Different configurations arising from the distribution of two In atoms in the supercell (A–C).

Table 1. Distance between the two In atoms in $SrTi_{0.75}In_{0.25}O_3$.

configuration	distance between the two In atoms
A	$\sqrt{3}a$
B	$\sqrt{2}a$
C	a

In our computation, the Perdew and Wang 91 parametrization is taken as the exchange-correlation potential in the generalized-gradient approximation (GGA). The cutoff energy of plane-wave is set at 420 eV; the maximum root-mean-square convergent tolerance is less than 2×10^{-5}eV/atom, that is, the energy and stress imposed on each atom are not greater than 0.1 eV and 0.1 GPa respectively. The Brillouin zone integration is approximated by using a special k-points sampling scheme of Monkhorst-Pack, and a $6 \times 6 \times 4$ k-points grid is used. All calculations are performed in reciprocal space. In order to obtain a stable structure, we optimize the atomic coordinate of doped $SrTiO_3$ by CASTEP geometry first. And then the electronic structure and optical properties are calculated based on the optimized supercell model.

3. Results and discussion

3.1. Electronic structure of In doped $SrTiO_3$

3.1.1. Density of states

In order to show the In doping effect on the electronic structure of $SrTiO_3$, the total (DOS) of stoichiometric $SrTiO_3$ are calculated first for comparison and the result is shown in Fig.2.

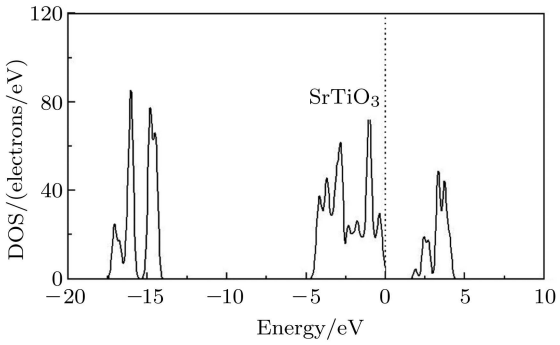


Fig.2. The DOS of $SrTiO_3$. The Fermi level is set to zero on the energy scale, which will be adopted below unless otherwise stated.

There exists an energy gap between the occupied O2p states and the unoccupied Ti 3 d states, which means that $SrTiO_3$ is an insulator with a Ti $3\,d^0$ electron configuration. The value of the band gap is about 1.6 eV, which is smaller than the experimental value of about 3.2 eV and the value of about 1.8 eV with the LMTO-ASA method in Ref.[17]. The reason for such a disagreement stems from the well-known shortcoming of the theory frame of DFT-LDA.[18]

Figure 3 shows the total DOSs of $SrTi_{1-x}In_xO_3$ with $x = 0.125$ and 0.25. Because the In doping introduces the p-type carriers into the system, the Fermi level shifts into the valence bands (VBs) for $x = 0.125$, which is in good agreement with the experimental results[13] that the $SrIn_{0.1}Ti_{0.9}O_3$ is a p-type semiconductor and the Fermi level shifts due to the substitution of In^{3+} for Ti^{4+}. At the same time, for the cases of $x = 0.125$ and 0.25, there are two additional peaks between the upper VBs and the lower VBs. One peak with a bandwidth of about 1.4 eV is located at the bottom of the upper VBs, the other with a bandwidth of about 1.2 eV lies above the lower VBs. And the two peaks intensify with the increase of In doping concentration. We will discuss these additional peaks later.

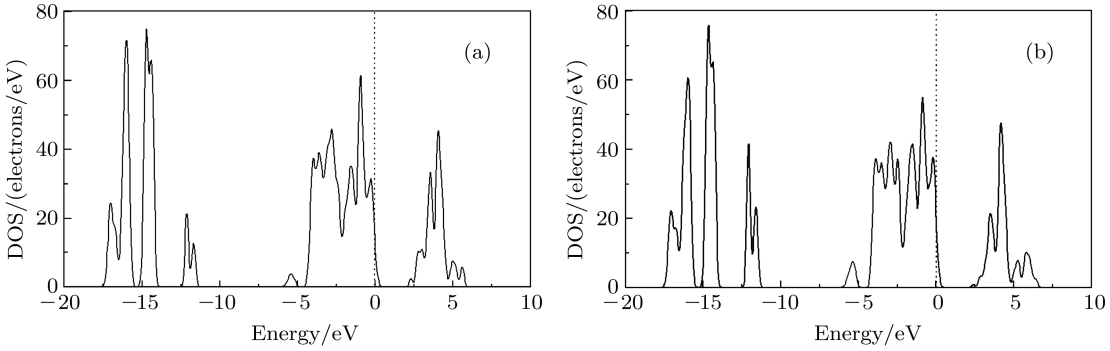


Fig.3. DOSs of $SrTi_{1-x}In_xO_3$ (a) $x = 0.125$; (b) $x = 0.25$.

In addition, the DOS shifts significantly towards high energies and the optical band gap broadens with the increase of In doping concentration compared with the DOS reported in Fig.2. The calculated optical band gap of $SrTi_{0.875}In_{0.125}O_3$ is about 0.35 eV larger than that of undoped $SrTiO_3$, which is well consistent with the experimental results that the band gap of $SrIn_{0.1}Ti_{0.9}O_3$ is 0.4 eV larger than that of pure $SrTiO_3$ due to In doping.[13] The reasons are as follows: on one hand, the Burstein–Moss shift due to the high concentration of carriers makes the optical absorption edge shift towards high energies, and the optical band gap is broadened;[19] On the other hand, interactions among hole charges result in a many-body effect, which causes the optical band gap to become narrow.[20] But the effect of Burstein–Moss on the band gap is more pronounced than the many-body effect, so the band gap broadens with the increase of In doping concentration.

The broadened optical band gap may be expressed by the following equation:

$$E_g = E_{go} + \Delta E_g^{BM} - \Delta E_g^{W}.$$

Here E_{go} is the band gap of undoped $SrTiO_3$, ΔE_g^{BM} is the Burstein–Moss shift and ΔE_g^{w} is the change of valence band resulting from the many-body effect among holes.

It should be noticed that although the Fermi level shifts downwards into the original VBs, there is no change in the topmost of the VBs and the bottom of conduction bands (CBs) in case of $SrTi_{1-x}In_xO_3$ with $x = 0.125$. This indicates that the rigid band model

is still valid for the $SrTiO_3$ with p-type doping when the doping concentration is not very high. However, there is significant change in the bottom of CBs when $x = 0.25$. It is due to the fact that Ti charge potential is greatly disturbed at a high amounts of In doping.

3.1.2. Partial density of states

Figure 4 shows the PDOSs of $SrTi_{1-x}In_xO_3$ at different amounts of In doping. The PDOS of doped $SrTiO_3$ has significant changes: an additional small peak appears in the bottom of the upper VBs, to which both the In5s state and O2p state can make contributions. And another large peak emerges above the lower VBs at the energy of about –12eV, to which In4d state makes a great contribution. Also, the PDOS shifts significantly towards high energies with the increase of In doping concentration, and the dispersion of the VBs is aggravated due to the high doping concentration that makes the impurity atoms become closer to each other. In this case, the wave functions which are bounded by the doping ions greatly overlap, resulting in the enhancement of the communization movement between the O2p orbit and the impurity atom orbit, so the VBs are broadened.

For the CBs, they are highly dispersive and show no localization characteristics with the increase of In doping. It is known that the effective radius of In^{3+} (0.094 nm) is larger than that of Ti^{4+} (0.0745 nm), the partial substitution of In for Ti has broken the Ti–O octahedra, which makes the unsubstituted Ti and O atoms squeeze into each other. This leads to a stronger hybridization between the Ti3d and O2p states, so the CBs become highly dispersive. Also the dispersion intensifies with the increase of In doping concentration.

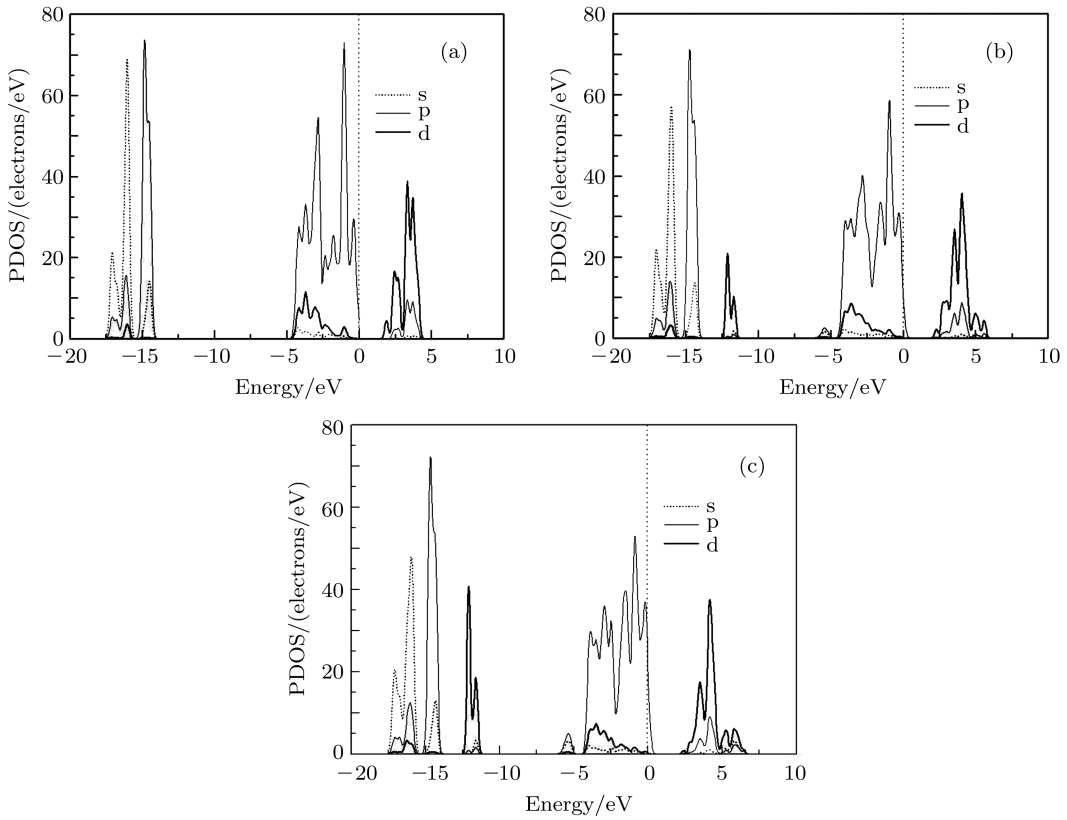


Fig.4. PDOSs of $SrTi_{1-x}In_xO_3$. (a) $x = 0.0$; (b) $x = 0.125$; (c) $x = 0.25$.

3.1.3. Electron density difference

Next, we discuss the In doping effect on the electronic structure of $SrTi_{1-x}In_xO_3$ in terms of the electron density difference. And the electron density difference of undoped $SrTiO_3$ is first calculated for comparison (see Fig.5(a)). It can be found that there is a strong covalency between Ti–O bonds, and the electron cloud near the Ti and O atoms indicates the orientation characteristic of covalency. After doping,

the electron density difference of $SrTi_{1-x}In_xO_3$ with $x = 0.125$ and 0.25 demonstrates a considerable electron charge density redistribution. The overlap of electron densities between Ti and O atoms is enhanced and the Ti–O covalency becomes strong with the increase of In doping concentration compared with that of undoped $SrTiO_3$. As for the In–O bond, it shows clear ionicity. At the same time, the electron clouds of Ti and O atoms shift towards high energies and the symmetry of the crystal reduces, which is consistent with the above discussed DOS and PDOS.

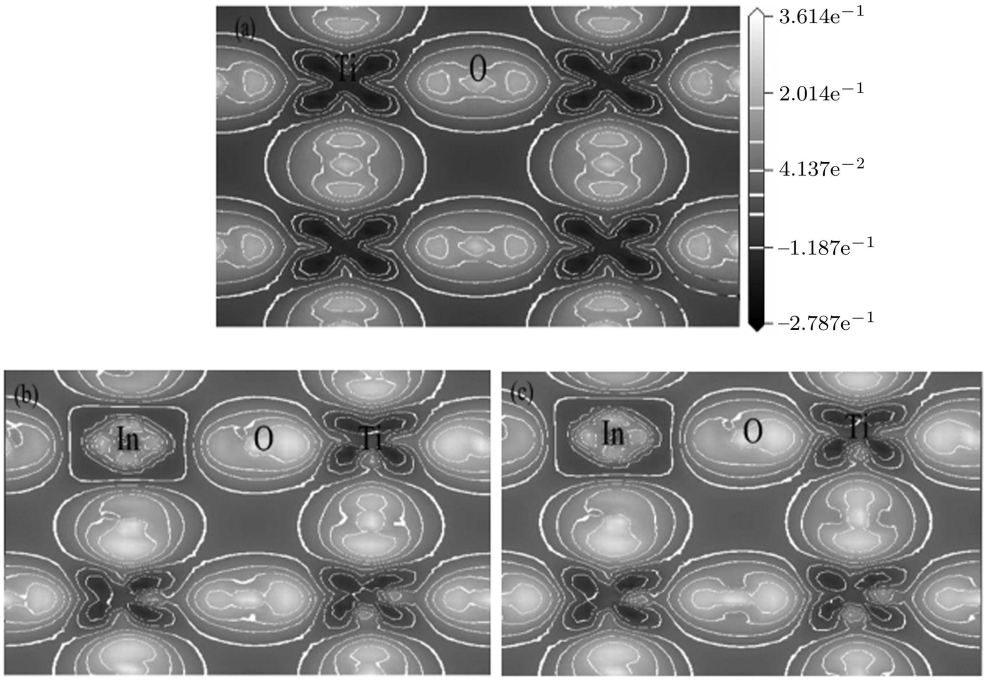


Fig.5. Electron density difference of $SrTi_{1-x}In_xO_3$ (a) $x = 0.0$; (b) $x = 0.125$; (c) $x = 0.25$.

3.2. The optical property of In doped $SrTiO_3$

Further insight into the effect of In doping on the electronic structure of $SrTiO_3$ can be obtained from the calculation of optical properties. The linear response of a system due to an external electromagnetic field with a small wave vector can be described with a complex dielectric function $\varepsilon(\omega) = \varepsilon_1(\omega) + i\varepsilon_2(\omega)$. The imaginary part of the dielectric function $\varepsilon_2(\omega)$ is calculated from the momentum matrix elements between the occupied and unoccupied wave functions[21] as follows:

$$\varepsilon_2(\omega) = \frac{Ve^2}{2\pi\hbar m^2\omega^2}\int \mathrm{d}^3k \sum_{n,n'} \langle kn|p|kn'\rangle|^2 f(kn)(1-f(kn'))\delta(E_{kn} - E_{kn'} - \hbar\omega), \tag{1}$$

where $\hbar\omega$ is the energy of the incident photon, V is the unit cell volume, p is the momentum operator, $|kn\rangle$ is a crystal wavefunction and $f(kn)$ is the Fermi distribution function. The real part of the dielectric function $\varepsilon_1(\omega)$ is evaluated from the imaginary part $\varepsilon_2(\omega)$ by the Kramers–Kronig relationship sa follows:

$$\varepsilon_1(\omega) = 1 + \frac{2}{\pi}M\int_0^\infty \frac{\varepsilon_2(\omega')\omega'}{\omega'^2 - \omega^2}\mathrm{d}\omega, \tag{2}$$

where M is the principal value of the integral. The other optical parameters like refractive index $n(\omega)$, extinction coefficient $k(\omega)$, reflectivity $R(\omega)$ and ab-

sorption coefficient $I(\omega)$ now immediately can be calculated in terms of the components of the complex dielectric function as follows:

$$n(\omega) = \frac{1}{\sqrt{2}}\left[\sqrt{\varepsilon_1(\omega)^2 + \varepsilon_2(\omega)^2} + \varepsilon_1(\omega)\right]^{1/2}, \quad (3)$$

$$k(\omega) = \frac{1}{\sqrt{2}}\left[\sqrt{\varepsilon_1(\omega)^2 + \varepsilon_2(\omega)^2} - \varepsilon_1(\omega)\right]^{1/2}, \quad (4)$$

$$R = \frac{(n-1)^2 + k^2}{(n+1)^2 + k^2}, \quad (5)$$

$$I = \frac{2K\omega}{c}. \quad (6)$$

Correspondingly the transmittance $T(\omega)$ can be obtained by the following equation:

$$T(\omega) = 1 - R(\omega) - I(\omega). \quad (7)$$

Figure 6 shows the transmittances of $SrTi_{1-x}In_xO_3$ with $x = 0.0$, 0.125 and 0.25. The transmittance of In doped $SrTiO_3$ has a significant improvement with the increase of In doping concentration, and the transmittance is higher than 85% in a wavelength range from 300 to 625 nm.

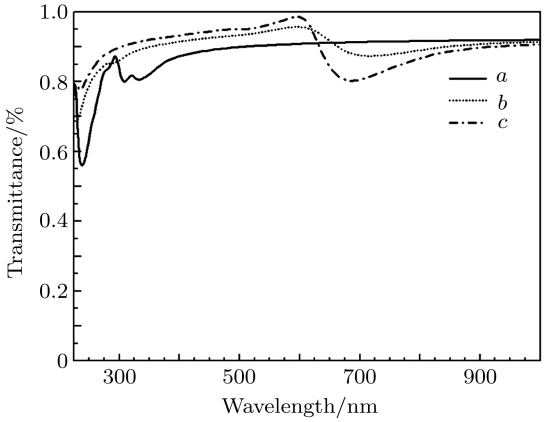


Fig.6. Optical transmittances of $SrTi_{1-x}In_xO_3$ (a) $x = 0.0$; (b) $x = 0.125$; (c) $x = 0.25$.

The increasing of high transparency originates from two factors. Obviously one is the wide optical band gap which broadens with the increase of In doping amounts. The other is the low PDOS of impurity In atom in the Fermi level (see Table 2). The PDOS of In atom is much lower than that of Ti atom, which leads to a small transition probability and weak absorption.

Table 2. The values of PDOS in the Fermi level with different In doping concentrations.

doping concentration	0.125	0.25
Ti(E_F)	0.103	0.242
In(E_F)	0.040	0.120

Moreover, the cut-off wavelength shifts into a blue-light region with In doping increasing. According to the Drude theory,[22] the relationship between the maximal plasma wavelength absorbed by free electrons and the carrier concentration can be described as

$$\frac{\partial\lambda}{\partial N} \angle 0,$$

where λ is the maximal plasma wavelength and N is the carrier concentration. As for transparent conducting films, they are highly reflective to electromagnetic waves with a long wavelength $\lambda_p(\lambda_p > \lambda)$ but highly transparent to those with a short wavelength $\lambda_p(\lambda_p < \lambda)$. That is to say, the cut-off wavelength in a visible region is determined by maximal plasma wavelength λ_p. Therefore the carrier concentration increases with In doping concentration increasing, and the cut-off wavelength shifts towards a blue region.

4. Conclusions

We have investigated the electronic structures including DOSs and PDOSs of $SrTi_{1-x}In_xO_3$ with $x = 0.0$, 0.125 and 0.25 by using the first-principles calculation of plane wave ultra-soft pseudo-potential based on the density function theory (DFT). Owing to the hole doping, the Fermi level shifts into valence bands (VBs) for $SrTi_{1-x}In_xO_3$ with $x = 0.125$ and the system displays the p-type degenerate semiconductor features. At the same time, the DOS shifts towards high energies and the optical band gap is broadened. The wide band gap, small transition probability and weak absorption due to the low PDOS of impurity in the Fermi level result in the optical transparency of the film. The optical transmittance of In doped $SrTiO_3$ is higher than 85% in a visible region, the transmittance improves greatly and the cut-off wavelength shifts into a blue-light region with the increase of In doping concentration. Owing to a lack of experimental results of the In-doped $SrTiO_3$ with different doping concentrations, further experimental investigation is required so that our theoretical results may be checked by the experimental results.

References

[1] Li H C, Si W D, West A D and Xi X X 1998 *Appl. Phys. Lett.* **73** 464

[2] Ernst F, Kienzle O and Ruhle M 1999 *J. Eur. Ceram. Soc.* **19** 665

[3] Pradhana A K, Sahu D R, Roul B K and Feng Y 2004 *J. Appl. Phys.* **96** 1170

[4] Uedono A, Shimayama K, Kiyohara M, Chen Z Q and Yamabe K 2002 *J. Appl. Phys.* **92** 2697

[5] Suzuki S, Yamamoto T, Suzuki H, Kawaguchi K, Takahashi K and Yoshisato Y 1997 *J. Appl. Phys.* **81** 6830

[6] Guo X G, Chen X S, Sun Y L, Sun L Z, Zhou X H and Lu W 2003 *Phys. Lett.* A **317** 501

[7] Tokura Y, Taguchi Y, Okada Y, Fujishima Y, Arima T, Kumagai K and Iye Y 1993 *Phys. Rev. Lett.* **70** 2126

[8] Fujimori A, Hase I, Nakamura M, Namatame H, Fujishima Y, Tokura Y, Abbate M, Groot F M F, Czyzyk M T, Fuggle J C, Strebel O, Lopez F, Domke M and Kaindl G 1992 *Phys. Rev.* B **46** 9841

[9] Higuchi T, Tsukamoto T, Kobayashi K, Ishiwata Y, Fujisawa M, Yokoya T, Yamaguchi S and Shin S 2000 *Phys. Rev.* B **61** 12860

[10] Zhang C 2007 *Chin. Phys.* **16** 1422

[11] Luo W D, Duan W H, Louie S G and Cohen M L 2004 *Phys. Rev.* B **70** 214109

[12] Cui D F, Wang H H, Dai S Y, Zhou Y L, Chen Z H, Yang G Z, Liu F Q, Kui R X and Qian H J 2002 *Acta Phys. Sin.* **51** 1029 (in Chinese)

[13] Dai S Y, Lu H B, Chen F, Chen Z H, Ren Z Y and Ng D H L 2002 *Appl. Phys. Lett.* **80** 3545

[14] Higuchi T, Tsukamoto T, Sata N, Ishigame M, Tezuka Y and Shin S 1998 *Phys. Rev.* B **57** 6978

[15] Huang H H, Shin S and Ishigame M 1991 *Solid State Ionics* **47** 251

[16] Segall M D, Lindan P J D, Probert M J, Pickard C J, Hasnip P J, Clark S J and Payne M C 2002 *J. Phys. Cond. Matt.* **14** 2717

[17] Guo X G, Chen X S and Lu W 2003 *Solid State Commun.* **126** 441

[18] Jones R O and Gunnarsson O 1989 *Rev. Mod. Phys.* **61** 689

[19] Burstein E 1954 *Phys. Rev.* **93** 632

[20] Mahan G D 1980 *J. Appl. Phys.* **51** 2634

[21] Saha S and Sinha T P 2000 *Phys. Rev.* B **62** 8828

[22] Ishiguro K, Sasaki J and Arai T 1958 *J. Phys. Soc. Japan* **13** 296